Acta Crystallographica Section E
Structure Reports
Online
ISSN 1600-5368

Rietveld refinement of $Ba_5(AsO_4)_3Cl$ from high-resolution synchrotron data

Anthony M. T. Bell,[a]* C. Michael B. Henderson,[b] Richard F. Wendlandt[c] and Wendy J. Harrison[c]

[a]Synchrotron Radiation Source, STFC Daresbury Laboratory, Daresbury, Warrington, Cheshire, WA4 4AD, England, [b]School of Earth, Atmospheric and Environmental Sciences, University of Manchester, Manchester, M13 9PL, England, and [c]Department of Geology and Geological Engineering, Colorado School of Mines, Golden, CO 80401, USA
Correspondence e-mail: a.m.t.bell@dl.ac.uk

Received 30 July 2008; accepted 20 August 2008

Key indicators: powder synchrotron study; T = 298 K; mean σ(As–O) = 0.040 Å; R factor = 0.059; wR factor = 0.082; data-to-parameter ratio = 22.1.

The apatite-type compound $Ba_5(AsO_4)_3Cl$, pentabarium tris[arsenate(V)] chloride, has been synthesized by ion exchange at high temperature from a synthetic sample of mimetite ($Pb_5(AsO_4)_3Cl$) with $BaCO_3$ as a by-product. The results of the Rietveld refinement, based on high resolution synchrotron X-ray powder diffraction data, show that the title compound crystallizes in the same structure as other halogenoapatites with general formula $A_5(YO_4)_3X$ (A = divalent cation, Y = pentavalent cation, X = Cl, Br) in space group $P6_3/m$. The structure consists of isolated tetrahedral AsO_4^{3-} anions (m symmetry), separated by two crystallographically independent Ba^{2+} cations that are located on mirror planes and threefold rotation axes, respectively. The Cl^- anions are at the 2b sites ($\bar{3}$ symmetry) and are located in the channels of the structure.

Related literature

For crystal chemistry of apatites, see: Mercier *et al.* (2005); White & ZhiLi (2003); Wu *et al.* (2003). For powder diffraction data on Ba-containing As-apatites, see: Kreidler & Hummel (1970); Dunn & Rouse (1978). Atomic coordinates as starting parameters for the Rietveld (Rietveld, 1969) refinement of the present phases were taken from Chengjun *et al.* (2005); Dai *et al.* (1991); de Villiers *et al.* (1971). For related Ba—Cl-apatites, see: Đordevic *et al.* (2008); Hata *et al.* (1979); Reinen *et al.*(1986); Roh & Hong (2005); Schiff-Francois *et al.* (1979). For synthetic work, see: Baker (1966); Essington (1988); Harrison *et al.* (2002).

Experimental

Crystal data

$As_3Ba_5ClO_{12}$
M_r = 1138.85
Hexagonal, $P6_3/m$
a = 10.5570 (1) Å
c = 7.73912 (8) Å
V = 746.98 (1) Å^3
Z = 2
Synchrotron radiation
λ = 0.998043 Å
μ = 56.07 (1) mm^{-1}
T = 298 K
Specimen shape: cylinder
40 × 0.7 × 0.7 mm
Specimen prepared at 100 kPa
Specimen prepared at 1258 K
Particle morphology: powder, white

Data collection

In-house design diffractometer
Specimen mounting: capillary
Specimen mounted in transmission mode
Scan method: step
Absorption correction: none
$2\theta_{\min}$ = 2, $2\theta_{\max}$ = 70°
Increment in 2θ = 0.01°

Refinement

R_p = 0.059
R_{wp} = 0.082
R_{exp} = 0.067
R_B = 0.090
S = 1.23
Excluded region(s): 2-6 degrees 2θ.
Profile function: Fundamental Parameters
464 Bragg reflections
21 parameters
Preferred orientation correction: none

Table 1
Selected geometric parameters (Å, °).

Ba1—O1	2.67 (5)	Ba2—O1^{v}	3.14 (4)
Ba1—O2^{i}	2.81 (4)	Ba2—Cl1^{iv}	3.281 (5)
Ba1—O3^{i}	3.12 (3)	As1—O3	1.64 (2)
Ba2—O2^{ii}	2.59 (4)	As1—O1	1.70 (8)
Ba2—O3^{iii}	2.62 (4)	As1—O2	1.70 (4)
Ba2—O3^{iv}	3.05 (4)		
O3—As1—O3^{vi}	118 (2)	O3—As1—O2	108 (2)
O3—As1—O1	108 (1)	O1—As1—O2	106 (2)

Symmetry codes: (i) $x - y, x, -z$; (ii) $-y + 1, x - y + 1, z$; (iii) $y, -x + y + 1, -z$; (iv) $x, y + 1, z$; (v) $-x + y, -x + 1, z$; (vi) $x, y, -z + \frac{1}{2}$.

Data collection: local software; cell refinement: *CELREF* (Laugier & Bochu, 2003); data reduction: local software; method used to solve structure: coordinates taken from a related compound; program(s) used to refine structure: *TOPAS* (Coelho, 2000); molecular graphics: *Balls and Sticks* (Kang & Ozawa, 2003); software used to prepare material for publication: *publCIF* (Westrip, 2008).

AMTB acknowledges the use of the EPSRC's Chemical Database Service at Daresbury (Fletcher *et al.*, 1996). AMTB also acknowledges the referees and Co-editor whose suggestions and comments helped to improve this paper.

Supplementary data and figures for this paper are available from the IUCr electronic archives (Reference: WM2188).

References

Baker, W. E. (1966). *Am. Mineral.* **51**, 1712–1721.
Chengjun, D., Xueyan, W., Wei, L., Haohong, C., Xinxin, Y. & Jingthai, Z. (2005). *J. Alloys Compd*, **396**, 86–91.
Coelho, A. (2000). *TOPAS*. http://members.optusnet.com.au/~alancoelho/.
Dai, Y.-S., Hughes, J. M. & Moore, P. B. (1991). *Can. Mineral.* **29**, 369–376.
Đordević, T., Šutović, S., Stojanović, J. & Karanović, Lj. (2008). *Acta Cryst.* C**64**, i82–i86.
Dunn, P. J. & Rouse, R. C. (1978). *Can. Mineral.* **16**, 601–604.
Essington, M. E. (1988). *Soil Sci. Soc. Am. J.*, **52**, 1566–1570.

Fletcher, D. A., McMeeking, R. F. & Parkin, D. J. (1996). *Chem. Inf. Comput. Sci.* **36**, 746–749.

Harrison, W. J., Wendlandt, R. F. & Wendlandt, A. E. (2002). International Mineralogical Association 18th General Meeting, Sept 1-6, 2002, Edinburgh, Scotland. Abstract A18-10, meeting program with abstracts, p. 185.

Hata, M., Marumo, F., Iwai, S. & Aoki, H. (1979). *Acta Cryst.* B**35**, 2382–2384.

Kang, S. J. & Ozawa, T. C. (2003). *Balls and Sticks.* http://www.softbug.com/toycrate/bs/index.html.

Kreidler, E. R. & Hummel, F. A. (1970). *Am. Mineral.* **55**, 170–184.

Laugier, J. & Bochu, B. (2003). *CELREF.* http://www.*CCP14*.ac.uk/tutorial/lmgp/*CELREF*.htm.

Mercier, P. H. J., Le Page, Y., Whitfield, P. S., Mitchell, L. D., Davidson, I. J. & White, T. J. (2005). *Acta Cryst.* B**61**, 635–655.

Reinen, D., Lachwa, H. & Allmann, R. (1986). *Z. Anorg. Allg. Chem.* **542**, 71–88.

Rietveld, H. M. (1969). *J. Appl. Cryst.* **2**, 65–71.

Roh, Y.-H. & Hong, S.-T. (2005). *Acta Cryst.* E**61**, i140–i142.

Schiff-Francois, A., Savelsberg, G. & Schaefer, H. (1979). *Z. Naturforsch. Teil B*, **34**, 764–765.

Villiers, J. P. R. de (1971). *Am. Mineral.* **56**, 758–766.

Westrip, S. P. (2008). *publCIF.* In preparation.

White, T. J. & ZhiLi, D. (2003). *Acta Cryst.* B**59**, 1–16.

Wu, P., Zeng, Y. Z. & Wang, C. M. (2003). *Biomaterials*, **25**, 1123–1130.

i64 Bell *et al.* • $As_3Ba_5ClO_{12}$ *Acta Cryst.* (2008). E**64**, i63–i64

supplementary materials

Acta Cryst. (2008). E**64**, i63-i64 [**doi:10.1107/S1600536808026901**]

Rietveld refinement of $Ba_5(AsO_4)_3Cl$ from high-resolution synchrotron data

A. M. T. Bell, C. M. B. Henderson, R. F. Wendlandt and **W. J. Harrison**

Comment

Apatites are minerals and synthetic compounds with general formula $A_5(YO_4)_3X$, containing tetrahedrally coordinated YO_4^{3-} anions (Y = pentavalent cation) and a monovalent anion X such as F^-, Cl^- or OH^-. The divalent cations frequently belong to the alkaline earth group, but other cations like Pb^{2+} are also known. For a review of the structures and crystal-chemistry of these materials, see Mercier *et al.* (2005) and White & Dong (2003). Apatites containing arsenic (As-apatites) are of interest as hosts for storage of arsenic removed from contaminated water (Harrison *et al.*, 2002). Powder diffraction data for the Ba containing As-apatites $Ba_5(AsO_4)_3Cl$ (Kreidler & Hummel, 1970) and for $(Ba_{2.25}Ca_{1.65}Pb_{1.16}Fe_{0.06}Mg_{0.06})[(AsO_4)_{2.56}(PO_4)_{0.3}]Cl_{1.09}$ (mineral name morelandite; Dunn & Rouse, 1978) were indexed in space group $P6_3/m$. Related crystal structures have also been reported for $Ba_5(AsO_4)_2SO_4S$ (Schiff-Francois *et al.*, 1979) and $(Sr_{1.66}Ba_{0.34})(Ba_{2.61}Sr_{0.39})(AsO_4)_3Cl$ (Dordevic *et al.*, 2008). The crystal structure of $Ba_5(AsO_4)_3Cl$ in space group $P6_3/m$ is reported in the present communication.

Table 1 shows refined interatomic distances and angles for the $Ba_5(AsO_4)_3Cl$ structure. The averaged Ba1—O and Ba2—O distances of respectively 2.87 Å and 2.84 Å are similar to those in other Ba and Cl containing apatites. In comparison, the average Ba1—O and Ba2—O distances are 2.84 Å and 2.78 Å for $Ba_5(VO_4)_3Cl$ (Roh & Hong, 2005), 2.83 Å and 2.79 Å for $Ba_5(PO_4)_3Cl$ (Hata *et al.*, 1979) and 2.83 Å and 2.76 Å for $Ba_5(MnO_4)_3Cl$ (Reinen *et al.*, 1986). The As—O distances are characteristic for tetrahedral AsO_4 units. The O—As—O angles deviate significantly from the ideal tetrahedral angle of 109.5°, indicating a strong distortion.

The refined lattice parameters for $Ba_5(AsO_4)_3Cl$ are similar to the previously published parameters of a = 10.54 Å, c = 7.73 Å given by Kreidler & Hummel (1970). A study of 108 existing and predicted apatites with different compositions made use of elemental radii to calculate their lattice parameters (Wu *et al.*, 2003). Only 52 of these compositions had known lattice parameters. The predicted lattice parameters for $Ba_5(AsO_4)_3Cl$ were a = 10.3979 Å, c = 7.6105 Å. These predicted parameters are respectively 1.51% and 1.66% smaller than the measured lattice parameters, and only 2 of the 52 apatite compositions had bigger differences between observed and calculated lattice parameters.

Fig. 1 shows the Rietveld difference plot for the present refinement. The crystal structure of $Ba_5(AsO_4)_3Cl$, showing the isolated tetrahedral AsO_4^{3-} anions separated by Ba^{2+} cations and Cl^- anions, is displayed in Fig. 2.

Experimental

This work was part of an attempt to synthesize analogues of $Pb_5(AsO_4)_3Cl$ (mimetite) with Pb^{2+} substituted by alkaline earth cations. All starting materials were well crystallized solids. $Pb_5(AsO_4)_3Cl$ was precipitated by titration of 0.1M Na_2HAsO_4 into a well stirred, saturated $PbCl_2$ solution at room temperature (procedure modified from methods of Baker (1966) and

Essington (1988)). The molar ratio of Pb:As was slightly greater than 5:3, allowing for excess $PbCl_2$ during the precipitation. A very fine-grained pure solid formed immediately, which was then separated, washed, and dried. Typically, five de-ionized water washes were needed to reduced the conductivity of the wash water to < 50 $\mu S \cdot cm^{-1}$. $Ba_5(AsO_4)_3Cl$ was successfully synthesized by ion exchange of $Pb_5(AsO_4)_3Cl$ with molten $BaCl_2$ at 1258 K (modified from the method given by Kreidler & Hummel (1970)). Two fusions were required to completely eliminate formation of Pb containing solid solutions and to yield the Pb free title compound. Excess metal in the form of $BaCl_2$ was removed from the solids by repeated washing with de-ionized water followed by centrifugation and filtration to separate the solid from the solution.

Refinement

The powdered sample was loaded into a 0.7 mm diameter borosilicate capillary, prior to high-resolution synchrotron X-ray powder diffraction data collection using station 9.1 of the Daresbury Synchrotron Radiation Source. The beam on the sample was 13 mm wide and 1.2 mm high. 9 powder datasets were collected, all were with a step with of 0.01°/2θ and a counting time of 2 s per point. Three of these datasets were collected between 5–70°/2θ, two between 30–70°/2θ, two between 40–70°/2θ, one between 31.73–70°/2θ and one between 2–13.2°/2θ. All of these data were summed and normalized to account for decay of the synchrotron beam with time. The main Bragg reflections of the powder diffraction pattern could be indexed in space group $P6_3/m$ with similar lattice parameters to those of the published powder diffraction data (Kreidler & Hummel, 1970). Some broad and weak Bragg reflections were matched by the pattern of $BaCO_3$ in space group *Pmcn*. The synchrotron X-ray wavelength was calibrated as 0.998043Å with an external *NIST* 640*c* silicon standard reference material.

Initial lattice parameters for the two phases were refined using *CELREF* (Laugier & Bochu, 2003). The $P6_3/m$ crystal structure of $Ba_5(PO_4)_3(OH)$ (Chengjun *et al.*, 2005) was used as a starting model for the Rietveld (Rietveld, 1969) refinement of the structure of $Ba_5(AsO_4)_3Cl$. The crystal structure of witherite (de Villiers *et al.*, 1971) was used as a starting model for refinement of the structure of $BaCO_3$. Isotropic atomic displacement parameters were used for both phases. For the $Ba_5(AsO_4)_3Cl$ phase the As—O distances in the AsO_4 tetrahedral units were constrained to those for mimetite (Dai *et al.*, 1991). For the $BaCO_3$ phase the C—O distances of the trigonal carbonate anion were constrained to those in witherite, and the U_{iso} factors for all atoms in the carbonate anion were constrained to be the same. As the $Ba_5(AsO_4)_3Cl$ phase was prepared by ion-exchange of $Pb_5(AsO_4)_3Cl$, Rietveld refinements were done with the metal sites partially occupied by both Pb and Ba. However, this resulted in the refined Pb occupancies falling to zero. Therefore the occupancies of the metal sites were fixed as fully occupied by Ba and no Pb was included for the final refinement of the $Ba_5(AsO_4)_3Cl$ phase. Proportions of the two phases were refined as 64.7 (9) wt.% $Ba_5(AsO_4)_3Cl$ and 35.3 (9) wt.% $BaCO_3$.

Figures

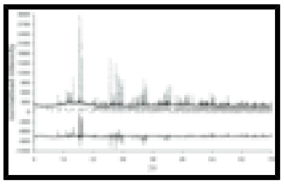

Fig. 1. Rietveld difference plot for the multi-phase refinement of $Ba_5(AsO_4)_3Cl$ and $BaCO_3$. The black dots, and grey and black lines show respectively the observed, calculated and difference plots. Calculated Bragg reflection positions are indicated by triangles for the $Ba_5(AsO_4)_3Cl$ phase and by crosses for the $BaCO_3$ phase.

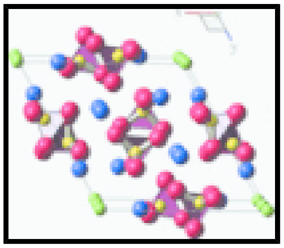

Fig. 2. The crystal structure of $Ba_5(AsO_4)_3Cl$. Pink tetrahedra show AsO_4 units with As^{5+} cations as yellow spheres and O^{2-} anions as red spheres. Large blue spheres represent Ba^{2+} cations and small green spheres Cl^- anions.

pentabarium tris(arsenate(V)) chloride

Crystal data

$As_3Ba_5Cl_1O_{12}$	$Z = 2$
$M_r = 1138.85$	$D_x = 5.063$ (1) Mg m^{-3}
Hexagonal, $P6_3/m$	Synchrotron radiation λ = 0.998043 Å
$a = 10.5570$ (1) Å	μ = 56.07 (1) mm^{-1}
$b = 10.5570$ (1) Å	$T = 298$ K
$c = 7.73912$ (8) Å	Specimen shape: cylinder
α = 90º	40 × 0.7 × 0.7 mm
β = 90º	Specimen prepared at 100 kPa
γ = 120º	Specimen prepared at 1258 K
$V = 746.98$ (1) Å^3	Particle morphology: powder, white

Data collection

In-house design diffractometer	$T = 298$ K
Monochromator: Si(111) channel-cut crystal	$2\theta_{min} = 2$, $2\theta_{max} = 70$º
Specimen mounting: capillary	Increment in 2θ = 0.01º
Specimen mounted in transmission mode	Increment in 2θ = 0.01º
Scan method: step	

Refinement

$R_p = 0.059$	Profile function: Fundamental Parameters
$R_{wp} = 0.082$	21 parameters
$R_{exp} = 0.067$	3 constraints
$R_B = 0.090$	?
$S = 1.23$	$(\Delta/\sigma)_{max} = 0.001$
Wavelength of incident radiation: 0.998043 Å	Preferred orientation correction: None
Excluded region(s): 2-6 degrees 2θ.	

Fractional atomic coordinates and isotropic or equivalent isotropic displacement parameters (Å^2)

	x	y	z	U_{iso}*/U_{eq}
Ba1	0.3333	0.6667	0.0061 (9)	0.059 (1)
Ba2	0.2445 (4)	0.9874 (6)	0.2500	0.065 (1)

As1	0.4047 (7)	0.3716 (7)	0.2500	0.059 (2)
O1	0.347 (7)	0.495 (6)	0.2500	0.13 (2)
O2	0.591 (4)	0.473 (4)	0.2500	0.08 (1)
O3	0.354 (2)	0.280 (3)	0.068 (3)	0.065 (8)
Cl1	0.0000	0.0000	0.0000	0.070 (6)

Geometric parameters (Å, °)

Ba1—O1$^{\mathrm{i}}$	2.67 (5)	Ba2—O3$^{\mathrm{vi}}$	2.62 (4)
Ba1—O1$^{\mathrm{ii}}$	2.67 (5)	Ba2—O3$^{\mathrm{vii}}$	3.05 (4)
Ba1—O1	2.67 (5)	Ba2—O3$^{\mathrm{viii}}$	3.05 (4)
Ba1—O2$^{\mathrm{iii}}$	2.81 (4)	Ba2—O1$^{\mathrm{ii}}$	3.14 (4)
Ba1—O2$^{\mathrm{iv}}$	2.81 (4)	Ba2—Cl1$^{\mathrm{viii}}$	3.281 (5)
Ba1—O2$^{\mathrm{v}}$	2.81 (4)	Ba2—Cl1$^{\mathrm{ix}}$	3.281 (5)
Ba1—O3$^{\mathrm{iv}}$	3.12 (3)	As1—O3	1.64 (2)
Ba1—O3$^{\mathrm{iii}}$	3.12 (3)	As1—O3$^{\mathrm{x}}$	1.64 (2)
Ba1—O3$^{\mathrm{v}}$	3.12 (3)	As1—O1	1.70 (8)
Ba2—O2$^{\mathrm{i}}$	2.59 (4)	As1—O2	1.70 (4)
Ba2—O3$^{\mathrm{iv}}$	2.62 (4)		
O3—As1—O3$^{\mathrm{x}}$	118 (2)	O3—As1—O2	108 (2)
O3—As1—O1	108 (1)	O3$^{\mathrm{x}}$—As1—O2	108 (2)
O3$^{\mathrm{x}}$—As1—O1	108 (1)	O1—As1—O2	106 (2)

Symmetry codes: (i) $-y+1, x-y+1, z$; (ii) $-x+y, -x+1, z$; (iii) $x-y, x, -z$; (iv) $y, -x+y+1, -z$; (v) $-x+1, -y+1, -z$; (vi) $y, -x+y+1, z+1/2$; (vii) $x, y+1, -z+1/2$; (viii) $x, y+1, z$; (ix) $-x, -y+1, z+1/2$; (x) $x, y, -z+1/2$.

Fig. 1

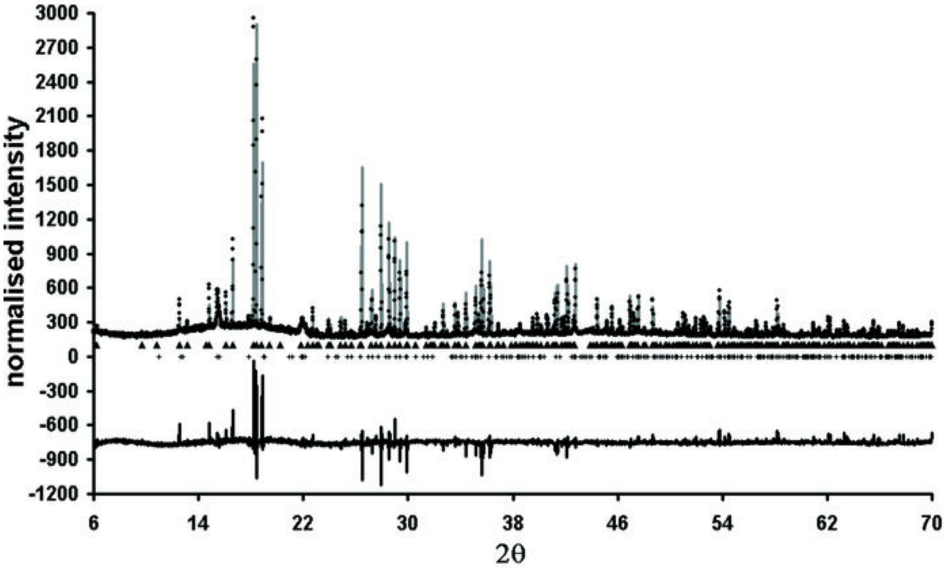
normalised intensity
3000
2700
2400
2100
1800
1500
1200
900
600
300
0
-300
-600
-900
-1200
6
14
22
30
38
46
54
62
70
2θ

Fig. 2